

Transcending the Limitation of Cosmetics: Ionic Liquids-inspired Novel Skin Penetration System as an Alternative to Medical Beauty Treatments

Anna Okishima*, Toru Okamoto, Tadao Fukuhara, Makoto Uyama, Reiji Miyahara, Tomoya Uchiyama;

MIRAI Technology Institute, Shiseido Co., Ltd., Yokohama, Japan

*Anna Okishima, 1-2-11, Takashima, Nishi-ku, Yokohama, 220-0011, Japan, +81-45-222-1600, anna.okishima@shiseido.com

Abstract

Increasing the amount of hydrophilic molecules in cosmetics that penetrate the skin improves the efficacy of cosmetic drugs by restoring skin function and increasing hydration. Because of the inherent tunability of molecule physicochemical properties such as melting point and hydrophobicity, both ionic liquids (ILs) and deep eutectic solvents (DESs) have attracted significant interest. Herein, we developed two types of “molecular modulation strategies” that were inspired by ILs and used to improve skin penetration of cosmetic active ingredients and enhance the cosmetic efficacy. (1) Incorporating penetration enhancers into ILs: Alkyl betaine (AB) was selected as a model of penetration enhancer. Of the material examined, AB-Xylitol (AB/XY) emerged as a liquidized enhancer that has higher penetration enhancement efficacy than AB alone. Following that, liquidation significantly reduced the toxicity tested by the assay using human epidermal keratinocytes. (2) Transforming drugs into ILs: The screening using 4-methoxysalicylic acid (4MS) as a model resulted in arginine (Arg) as the counter ion that generates 4MS IL. Interactions between 4MS carboxyl ion and Arg carboxyl ion and amine were confirmed by NMR spectroscopy. The effectiveness of drug penetration amounts was then demonstrated by Franz diffusion cells. 4MSK-ArgHCl revealed dramatically higher permeability compared to 4MSK alone. Using these insights, molecular modulation strategies have the potential to greatly alter the character of a molecule simply by mixing it. Furthermore, cosmetics that use these strategies can help consumers stay healthy, beautiful, and age-free.

Keywords: Skin Penetration; Active drug; Ionic Liquids; Deep eutectic solvents; Skin effect.

1. Introduction.

Active drugs in cosmetics play an important role in improving skin functions such as elasticity and moisture; however, the majority of drugs used in cosmetics are hydrophilic, ionic, and have a high melting point. These drugs have a low partition coefficient against the highly hydrophobic skin and diffusion coefficient in the skin. As a result, they have little chance of reaching the active site, such as the epidermis, and their effect is not as good as the consumer expected. For these reasons, the development of novel strategies to improve drug skin penetration is required.

For example, manipulating chemical properties by the conjugation of functional groups has been used to improve the skin penetration amounts of hydrophilic drugs [1]. However, because of the acceptance of safety assurance, developing novel ingredients for cosmetics takes time and money. Furthermore, although several studies have shown that penetration enhancers improve hydrophilic drug diffusion by disrupting the stratum corneum structure, it may cause skin irritation. [2-3].

Hence, we focused on ionic liquids (ILs) and deep eutectic solvents (DESs), which have recently shown great potential as drug delivery methods for the absorption of drugs that is difficult to penetrate the body [4-7]. ILs are salts that are melted below 100°C and are made up of asymmetric cations and anions [8]. DESs are co-fused mixtures of at least two components, one of which is a hydrogen bond donor compound and one of which is a hydrogen bond acceptor compound, and have a lower melting point than either of the original components [9]. For the sake of simplicity, DESs are also referred to collectively as ILs hereafter. ILs have functions in which the physicochemical properties of the molecule, such as melting point, diffusion, and distribution, can be arbitrarily manipulated by appropriately combining dissimilar molecules. The present study demonstrated the potential of “molecular modulation strategies” to be utilized for the enhancement of cosmetic drug efficacy by increasing the amounts of drugs in active sites.

In this study, the potential of ILs inspired us an idea of molecular modulation strategies. These approaches can improve the physicochemical properties of drugs without changing their chemical structures. Based on these findings, we attempted to improve active drug penetration by “incorporating penetration enhancers into ILs” and “transforming drugs into ILs.” Alkyl betaine (AB) was chosen as a model for “incorporating penetration

enhancers into ILs.” Penetration enhancer IL containing AB significantly enhance the penetration of model drug, 4-methoxysalicylic acid (4MS), compared with AB alone. Furthermore, the penetration enhancer ILs were investigated in terms of skin irritation reduction. 4MS was also selected as a model for “transforming drugs into ILs.” Its potassium salt is used as a brightening agent; however, it is highly hydrophilic ($\text{Log}P = -2.21$; pH = 7). A variety of counter ion have been screened for the fluidizing effect of 4MS. Among these, arginine (Arg)-4MS was chosen as a drug ILs for concept demonstration and demonstrated skin penetration effect. Over all, our strategies improved skin permeation significantly, which has great potential in cosmetic active drug delivery.

2. Materials and Methods.

2.1. Materials

The following materials were obtained from commercial sources: 4-methoxysalicylic acid (4MS) and L-carnitine from Tokyo Chemical Industry Co., Ltd. (Tokyo, Japan); methanol from Nacalai Tesque, Inc. (Kyoto, Japan); L-histidine and L-lysine from Kanto Chemical Co., Inc. (Tokyo, Japan); L-citrulline, phosphate-buffered saline (PBS) and trypsin from FUJIFILM Wako Pure Chemical Co. (Osaka, Japan). Other ingredients in this study were cosmetic grade and used without purification.

2.2. Preparation of IL and IL incorporating AB

In methanol aqueous solution (weight fraction of water/methanol = 1:1), 4MS was stirred in the presence of its counter ion candidates as well as AB thoroughly in the dark for 24 hours at 50°C. The excess water and ethanol were then removed by vacuum evaporation at 50°C

2.3. Characterization

2.3.1. Differential Scanning Calorimetry (DSC)

DSC was performed on a TA2000 (Mettler-Toledo International Inc., Zurich, Switzerland) using a scanning rate of 5°C/min. The sample size was 4.5–5.5 mg. For ILs, two heating and cooling cycles were performed, and the second heating cycles were analyzed to allow removal of residual water during the first heating cycle.

2.3.2. Fourier Transform Infrared (FT-IR) Spectroscopy

The FT-IR spectra of ILs were collected using a Nicolet iS50 FT-IR (Thermo Fisher Scientific, Inc., Waltham, MA, USA) in attenuated reflectance (ATR) mode. The final spectrum is the average of 32 individual scans, obtained within the range from 4400 to 800 cm^{-1} and resolution of 4 cm^{-1} .

2.3.3. NMR Spectroscopy

^{13}C -NMR measurements were performed with a JNM ECA-600 spectrometer (JEOL, Co., Ltd., Tokyo, Japan). A 1wt% D_2O solution of Sodium 3-(trimethylsilyl) propionate was used as an external standard whose trimethyl signal is 0 ppm. To obtain ^{15}N -NMR signals, PFG ^1H - ^{15}N -HMBC was measured, which conditions were direct axis data points = 2048, indirect axis data points = 256, scan number = 256, long-range ^1H - ^{15}N J coupling constant= 8Hz, and repetition time = 2 sec.

2.4. Skin Penetration Study

2.4.1. In Vitro Diffusion Study

The skin penetration studies were undertaken using Strat-M[□] (Merck Millipore, Billerica, MA, USA) as a model membrane in Franz diffusion cells (membrane area = 2.27 cm^2). 1 mL of each sample was applied to the membrane, and 9.6 mL of phosphate buffer saline (PBS, pH 7.4) was placed in the receptor compartment. The membrane was maintained at $32^\circ\text{C} \pm 1^\circ\text{C}$ while the PBS was stirred continuously using a magnetic stirrer. The drug concentrations in the receptor compartment were then analyzed using liquid chromatography-mass spectrometry with photodiode-array detection (254 nm), and the total amount of 4MS penetrated and flux values were calculated using the previously described methods [10].

2.4.2. In Vitro Skin Penetration Study

In vitro, skin penetration studies were performed using a flow diffusion cell array system (Introtec, Kanagawa, Japan). The diffusion surface area was 0.785 cm^2 . Analytical Biological Services Inc. (Wilmington, DE, USA) provided the human skin. Skin samples of 5 $\mu\text{L}/\text{cm}^2$ were applied. PBS was placed in the acceptor compartment (pH 7.4). The skin

surface temperature was maintained at around 32°C. Samples from the receptor compartment were taken 1, 2, or 4 hours after application. The skin layers were then separated. The drug concentrations were determined using LC-MS (liquid chromatography- mass spectroscopy, Shimadzu. Co., Kyoto, Japan). Shiseido Research Ethics Committee has approved the purchase and use of human skin

2.5. Cytotoxicity Studies

2.5.1. Cell Culture

Normal human epidermal keratinocytes (NHEK; ATCC, Manassas, VA, USA) were maintained in EpiLife medium (Thermo Fisher Scientific Inc.) supplemented with HuMedia-KG containing growth factors (Kurabo Inc., Osaka, Japan) and 60 µmol/L CaCl₂. Cells were cultured at 37°C in a humidified atmosphere with 5% CO₂.

2.5.2. Cytotoxicity Assay

NHEK cell line seeded at 8 × 10⁴ cells/well in 24-well plates. Cytotoxicity was assessed by the Alamar Blue assay [11]. Alamar Blue Cell Viability Reagent was from Thermo Fisher Scientific Inc. The cells were exposed to a medium containing vehicle (control), 25 mmol/L AB, or 25 mmol/L AB and 100 mmol/L XY for 24 hours after seeding. After the samples were removed, the well plates were placed in the incubator for another 18 hours under the same conditions but in simple medium. 3 hours before the absorbance measurements, cells were exposed to the resazurin compound and returned to the incubator. The results presented as% cell viability (mean ± standard deviation, n = 4) calculated according to Equation (1)

$$\text{cell viability} = \frac{\text{Abs. read in sample cells}}{\text{Abs. read in control cells}} \times 100 \quad (1)$$

2.6. Stratum Corneum (SC) Studies

2.6.1 SC Preparation

The SC layers were prepared as previously reported [12]. Human skin (50 years old, male, from Analytical Biological Services Inc.) was soaked in a 60°C-water bath for 3 min before being immersed in PBS containing 0.1% trypsin for 1 hour to remove the epidermis cells attached to the SC. Following that, the skin was thoroughly washed with PBS and

purified water to remove the epidermis cell. SCs were kept until they were needed. Shiseido Research Ethics Committee has approved the purchase and use of human skin

2.6.2. *SC Measurements*

SC was immersed in water containing 6.25, 12.5, 25 mmol/L AB and 25, 50, 100 mmol/L XY for 24 hours and washed with ultra-pure water, and dried for 12 hours. Spectra of dried SC were taken as shown in 4.3.2.

3. Results.

3.1. Incorporating Penetration Enhancers into ILs

3.1.1. *Enhancer IL Screening*

AB, which has been shown to improve penetration [13], was chosen, and the change in mechanism of action caused by conversion to IL was investigated according to the previous article [2]. ILs were prepared via heating method as previously described [14].

Table 1 shows the results of visual observation of IL formation when mixed with AB at various molar ratios, and IL formation was confirmed visually at room temperature. As a result, AB/XY was used in this study as a prototype of the penetration enhancer IL for further investigation, with XY expected to improve skin.

3.1.2. *Enhancer IL Characteristics*

The intermolecular interaction of the IL, AB-Xylitol (AB/XY) at a molar ratio of 1:3, was confirmed by ATR FT-IR (**Figure 1a**). In the AB spectrum, 1627 cm^{-1} is assigned to the amide I peak, and 1605 cm^{-1} is assigned to the asymmetric stretching vibration of COO^- . On the other hand, in the AB/XY spectrum, the peak at 1605 cm^{-1} was shifted to 1627 cm^{-1} and overlapped with the amide I band. Also, the peak at 2916 cm^{-1} and 2853 cm^{-1} assigned to CH_2 symmetry and asymmetry stretching in the AB spectrum was shifted to 2922 cm^{-1} and 2853 cm^{-1} , respectively, in the AB/XY spectrum. In addition, the C-N stretching vibration at 1334 cm^{-1} was shifted to 1325 cm^{-1} in AB. In the XY spectrum, the C-OH stretching vibration was shifted from 1004 cm^{-1} to 1040 cm^{-1} . $^{13}\text{C-NMR}$ also showed that the carbon peak attributed to AB COO^- was shifted to the lower field side.

The glass transition temperature at -32°C was determined by DSC (**Figure 1b**).

Table 1 | Screening of Conformer for Creating ILs with AB

Type	Chemicals	Ratio of ingredients to AB (molar ratio as a chemical) and visual aspect ^a			
		0.5	1	2	3
Organic acid	Lactic acid	S	S	TL	TL
	Salicylic acid	S	S	S	S
	Citric acid	S	S	TL	TL
Amino acid	Lysin-HCl	S	S	S	S
	Arginine	S	S	S	S
	Arginine-HCl	S	TL	TL	-
	Alanine	S	S	S	-
	Hydroxyproline	S	S	S	S
	Glutamic acid	S	S	S	S
	Glycine	S	S	S	S
	Serine	S	S	S	S
	Aspartic acid	S	S	S	S
Polyol	Glycerol	S	S	S	TL
	Erythritol	S	S	NS	NS
	Xylitol	S	S	TL	TL
	Sorbitol	S	S	TL	TL
	1,3-Butylene glycol	S	TL	TL	TL

^aTL: Transparent liquid, S: Solid present, NS: Liquid with low stability (<1 week)

As a screening, the combinations that result in a transparent liquid were chosen

3.1.3. Penetration Enhancement Effect of AB/XY

In a human skin penetration study (**Figure 2a**), the addition of AB/XY at a molar ratio of 1:4 at a dose of 25 mmol/L as AB resulted in a 4.3-fold higher accumulation of 4MSK in the epidermis after 4 hours compared to the control and 1.8-fold higher than AB alone (**Figure 2b**). Surprisingly, the toxicity of AB/XY was also assessed using epidermal cells and found to be significantly lower than that of AB alone (**Figure 2c**).

3.1.4. Mechanisms of Action

To investigate the mechanism of penetration enhancement, SC sheets were immersed in aqueous solutions of AB/XY (10, 20, 25, mmol/L as AB concentrations) at a molar ratio

of 1:4, and IR spectra were taken. After 24 hours of immersion, the peak intensity of the CH₂ symmetric and asymmetric stretching was reduced (**Figure 3a**). Furthermore, the CH₂

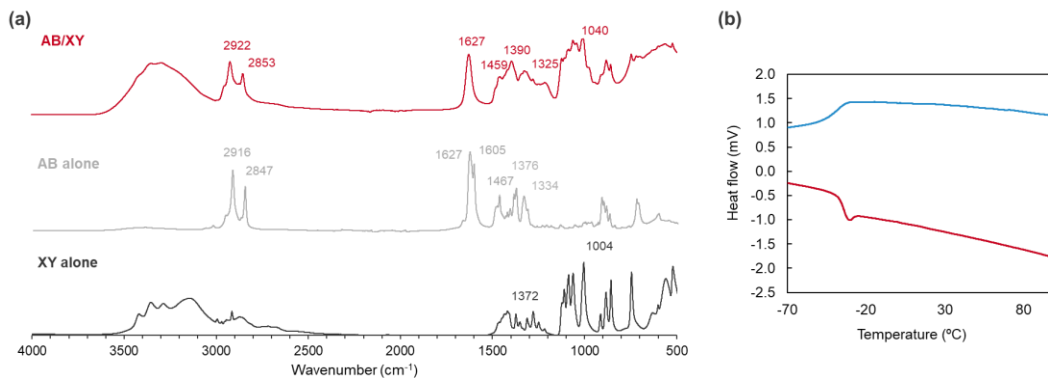


Figure 1 | Characteristics of AB/XY.

(a) FT-IR spectra of AB/XY (red line), AB (gray line), and XY (black line). Absorption peaks with numerical values are peaks shifted by IL production. The formation of ILs shifted the peaks of carbonyl and alkyl groups in AB, implying that AB and XY interact via those sites. (b) DSC chart of AB/XY at a molar ratio of 1:3. The blue line represents the cooling thermal behavior, while the red line represents the second heating thermal behavior. Peaks rising above the baseline represent endothermic peaks. The heating rate was 5°C/min. Baseline shift indicates glass transition.

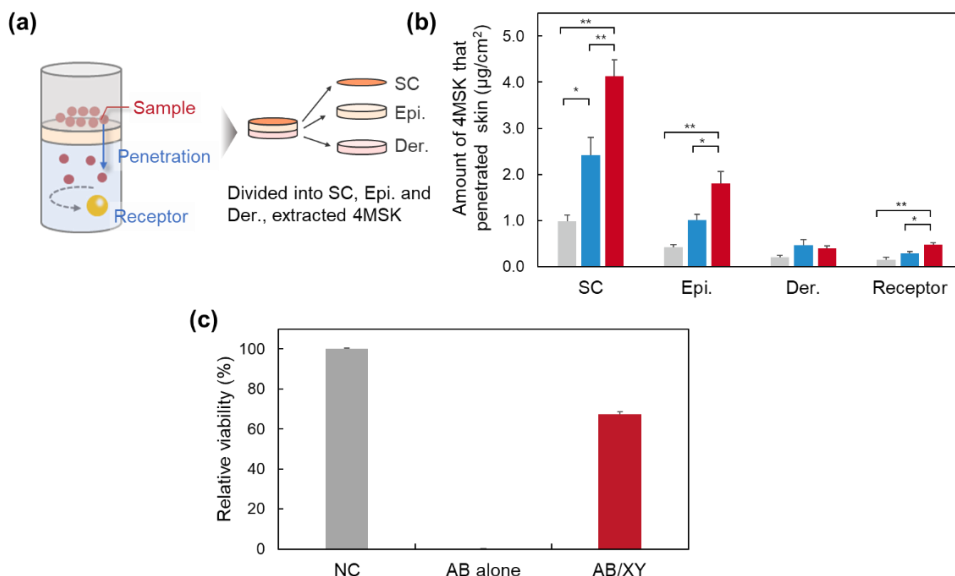


Figure 2 | Effect of making AB IL on penetration enhancement effect and toxicity.

(a) Illustration of the experiment protocol and (b) amount of 4MSK into and across the skin after topical application from control (gray), 25 mmol/L AB alone (blue), and 25 mmol/L AB and 100 mmol/L XY (red) aqueous solution. Data represents mean \pm 1 S.E., n = 6. *P < 0.05, **P < 0.01, a significant difference (Tukey's HSD test) Epi.: Epidermis, Der.: Dermis. (c) Viability of keratinocytes after being exposed to samples. Cellular toxicity with AB alone or AB/XY (25 mmol/L as alkyl betaine) observed when incubated with human epidermal keratinocytes (NHEK cells) for 24 h. Each bar represents mean \pm S.E. (n = 4)

asymmetric stretching vibrations of intercellular lipids in the SC derived from fatty chains showed a concentration-dependent high wavenumber shift of AB/XY (**Figure 3b**). On the other hand, there was no change in the CH₂ scissoring bands.

3.2. Transforming Drugs into ILs

3.2.1. Screening of Drug ILs

First, as shown in **Table 2** and **Figure 4a**, ILs composed of 4MS and each counter ion candidate were synthesized according to previous work [15], and the morphology after solvent volatilization was observed. As a result, when 4MS was combined with compounds containing quaternary ammonium salts and some basic amino acids, the mixture became liquid at room temperature (**Figure 4b**).

3.2.2. Skin Penetration Enhancement Effect of Drug ILs

Before the skin penetration test, 4MSK-penetration speeds were observed by an *in vitro* diffusion experiment in an infinite dosing system with Strat-M® as a model membrane (**Figure 5a**). Penetration fluxes were calculated from the slope at a steady state. As indicated by the flux values, simply combining 4MSK and ArgHCl increased the 4MSK-penetration speed by a factor of 2.5 (**Figure 5b**). **Figure 5c-e** show the results of the actual distribution of 4MSK in the human skin at 1, 2, and 4-hour(s) after application. They were measured by *in vitro* penetration test using human skin. The concentration of 4MSK in the SC, epidermis, and dermis increased significantly in the presence of ArgHCl 1 hour after application. After 2 and 4 hours, the concentrations in the skin were found to increase continuously.

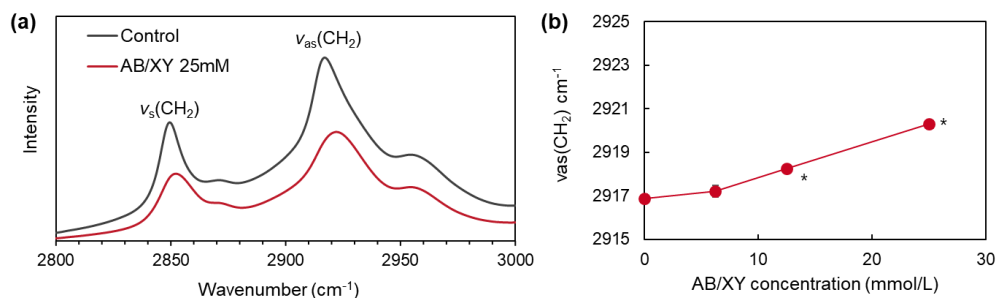


Figure 3 | AB/XY penetration enhancement mechanisms.

(a) ATR-FTIR spectra for SC samples after 24 h incubation in water or 25 mmol/L AB/XY (1:4) in a high wavenumber region. (b) The dose-depending position of CH₂ asymmetric stretching peak. Data represents mean \pm 1 S.D., n = 4. *P < 0.05 significant difference vs. 0 mmol/L (Dunnett's test)

Table 2 | Summary of 4MS-IL screening

Coformer	Molar ratio	Visual aspect ^a
Choline	1:1	TL
Trimethylglycine	1:1	TL
L-Carnitine	1:1	TL
L- Citrulline	1:1	S
L-Arginine	1:1	TL
	1:2	TL
	1:3	TL
L-Lysine	1:1	S
L-Histidine	1:1	TL
Nicotinamide	1:1	S
Caffeine	1:1	S

^aTL: Transparent liquid, S: Solid present

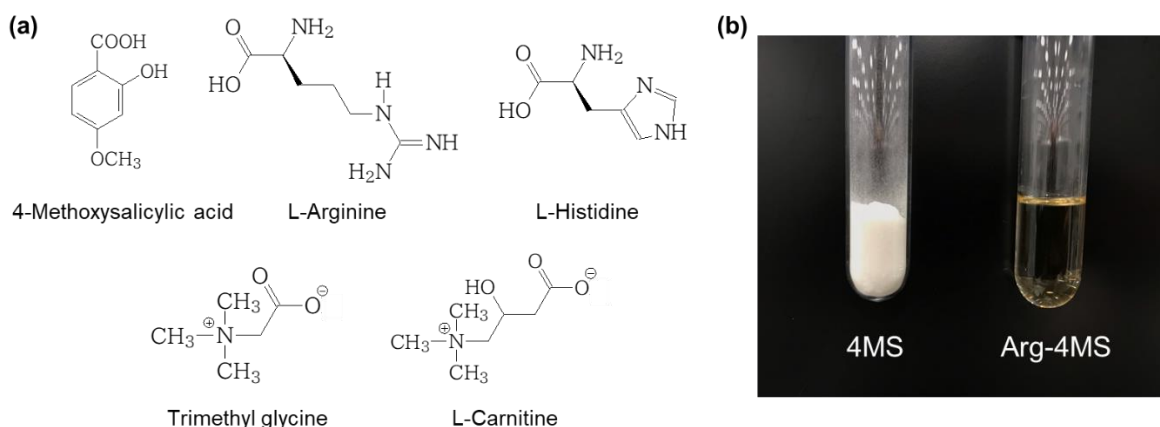


Figure 4 | Screening of compounds that makes 4MS IL.

(a) Structures of 4MS and the counterions. (b) Visual images of 4MS and Arg-4MS IL. The RT-ILs were obtained.

3.2.3. Characteristics of IL containing Drug

Arg-4MS was selected out of the liquidized systems for detailed physical property analysis. First, NMR measurements of Arg-4MS were performed. In **Figure 6a** ^{13}C -NMR spectra at 30°C of 1.9wt% 4MS $\text{D}_2\text{O}/\text{CD}_3\text{OD} = 9/7$ solution, 50wt% Arg D_2O solution, and Arg-4MS are shown. In **Figure 6b**, ^{15}N axis projection data of $^1\text{H}-^{15}\text{N}$ -HMBC spectrum at 30°C of 50wt% Arg D_2O solution and Arg-4MS NEAT, meaning IL alone without dilution, are shown. From these data, the subtraction of chemical shifts from 4MS or Arg to Arg-4MS was calculated and summarized in **Figure 6c**. ^{13}C -NMR spectra revealed that the chemical

shifts of carbons 1 and 3 in Arg were shifted to higher fields, while carbons 1 and 7 in 4MS were shifted to lower fields.

To determine the molar ratio of 4MS to Arg ion pairs in the Arg-4MS NEAT, ^{13}C -NMR spectra at 70°C of various IL samples with 4MS to Arg molar ratios of 1:1, 1:2, and 1:3 were taken. The 4MS signal was almost completely unshifted, but the first carbon of Arg was shifted to lower fields. When the molar ratio of 4MS to Arg exceeds 1:1, the presence of

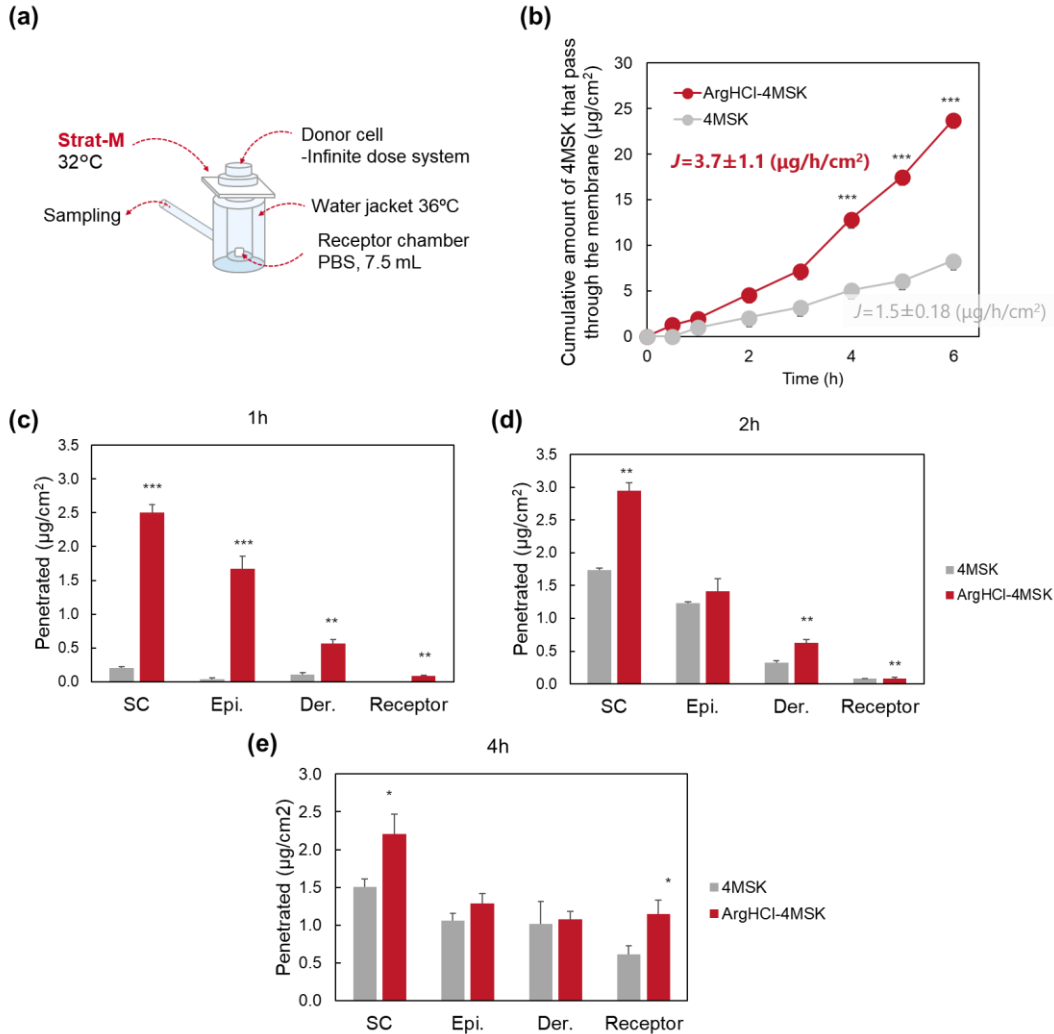


Figure 5 | Enhancement effect of ArgHCl on 4MSK penetration.

(a) Illustration of the *in vitro* diffusion experiment. (b) Penetration profile of 4MSK through Strat-M. The pH of the samples was adjusted to 5.5. Penetration fluxes (J) were obtained from the slope of the approximated line from 2h to 4h. Each point represents mean \pm 1 S.D., $n = 4$. (c-d) Time course of the 4MSK penetration and distribution. Distribution of 4MSK in the skin and receptor at (c) 1, (d) 2, and (e) 4-h after application. Data represents mean \pm 1 S.E., $n = 6$. * $P < 0.05$, ** $P < 0.01$, *** $P < 0.001$, significant difference (Student's *t*-test).

Arg molecules is indicated by these NMR spectra (data not shown) Following that, ATR-IR measurements of 4MS alone, Arg alone, and Arg-4MS revealed the disappearance of asymmetric stretching of non-free carboxyl groups observed at 1642 cm^{-1} in 4MS and a free carboxylic acid peak at 1585 cm^{-1} in Arg-4MS (**Figure 6d**). The C=O stretching peak observed at 1548 cm^{-1} in Arg alone was shifted to 1558 cm^{-1} in Arg-4MS. These IR data fully supported NMR data.

The melting point was determined by DSC and Arg-4MS 1:1 has a glass transition temperature near 0°C .

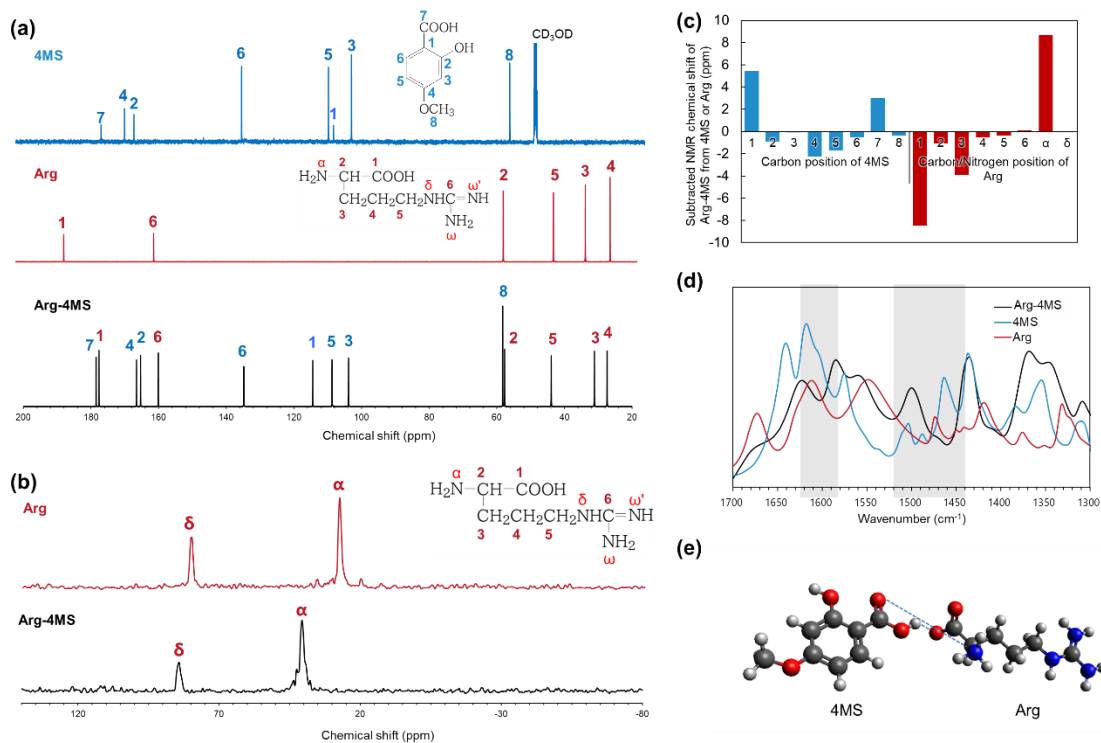


Figure 6 | Characterization of Arg-4MS.

(a) ^{13}C NMR spectra at 30°C of 1.9wt% 4MS D₂O/CD₃OD = 9/7 solution (blue line), 50wt% Arg D₂O solution (red line), Arg-4MS NEAT (black line). **(b)** ^{15}N axis projection data of ^1H - ^{15}N HMBC spectrum of 50wt% Arg D₂O solution (red line), Arg-4MS NEAT (black line). **(c)** Summary of subtracted NMR chemical shift of Arg-4MS from 4MS or Arg. **(d)** Overlapped ATR FT-IR spectra of Arg-4MS, 4MS and Arg. **(e)** Interaction between 4MS and Arg

The ^{13}C -NMR spectrum at 30°C of NEAT Arg-4MS and 50wt% D₂O solution of mixture 4MS-K and Arg-HCl which the molar ratio of 4MS-K to Arg-HCl is 1:1 are shown in **Figure 7**. Because all of the corresponding signals in these NMR spectra had nearly the

same chemical shift, it is suggested that 4MS and Arg formed the same IL with Arg-4MS in spite of being in the 4MS-K/Arg-HCl (ArgHCl-4MSK) solution.

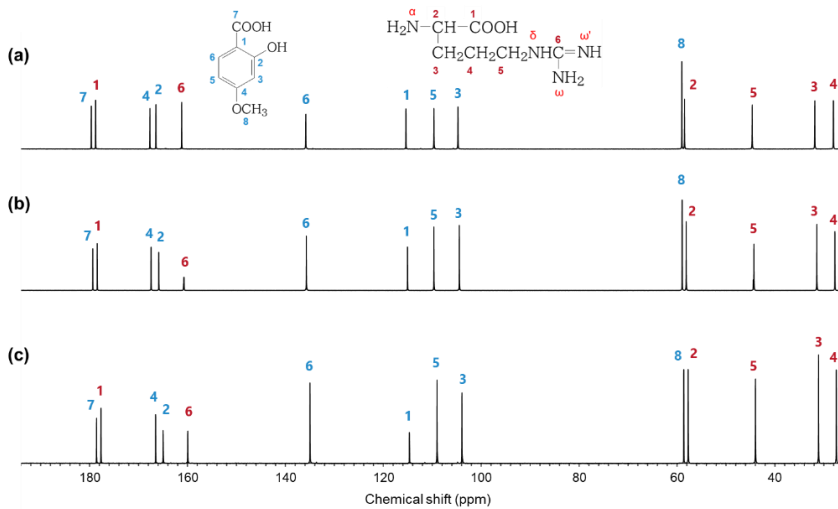


Figure 7 | Characterization of the solution state IL.

^{13}C -NMR spectra of (a) Arg-4MS NEAT, (b) 50wt% D_2O solution of 4MS and Arg which molar ratio is 1:1, (c) 50wt% D_2O solution of 4MS-K and Arg-HCl which molar ratio is 1:1.

4. Discussion.

We devised a molecular modulation strategy based on IL theory to improve skin penetration of drugs and penetration enhancers without compromising their properties, and we used 4MS as a model compound. The potassium salt of 4MS is used as a brightening agent, but its activity is frequently underutilized because its high water solubility prevents it from penetrating the SC [16].

4.1. Incorporating Penetration Enhancers into ILs

First, we challenged ourselves to create a safer and more effective penetration enhancer by converting it to an IL. We chose AB as a model because it is known to enhance penetration via SC fluidization and lipid extraction, but there are safety concerns [2]. Polyols have already been reported to form ILs in combination with betaine; Kamarza *et. al.* stated that the carboxy groups of betaine and the hydroxy groups of 1,4-butanediol form hydrogen bonds [17]. The formation of ILs with AB was observed in all polyols tested in the current study. ATR FT-IR and DSC measurements were performed as a confirmatory experiment for

interaction and IL formation. In ATR FT-IR spectra, the peak of the AB COO⁻ and CH₂ were shifted. Furthermore, the XY C-OH peak was shifted. These results indicate the hydrogen bonding between COO⁻, CH₂, and CH₃ of AB and -OH group of XY [18]. The NMR data agrees with the ATR FT-IR data. DSC measurements also revealed that AB/XY is amorphous with a glass transition temperature. This is consistent with several ILs having glass transition temperatures [19-20].

In the transdermal permeation experiments, the penetration of 4MSK was significantly enhanced by using AB/XY compared with AB alone, suggesting that the action of AB was enhanced by converting it to an IL; Furthermore, it can be concluded that, in terms of the toxicity test, our strategy allows penetration enhancers to avoid causing skin irritation in consumers. Polar groups are known to cause AB cytotoxicity [21], and the sealing of polar groups by ILs in this study may have contributed to the reduction of toxicity and enhancement of effect. In terms of the mechanism of action of AB/XY on the stratum corneum, the peak intensity of the CH₂ symmetric and asymmetric stretching was reduced, suggesting that the drug has an effect that extracts lipids from the SC. This change is similar to the previously reported mechanisms of ILs [22]. The concentration-dependent high wavenumber shift of AB/XY was observed in the fatty chain-derived CH₂ asymmetric stretching vibration of intercellular lipids in SC. This indicates an increase in SC lipid structure disorder associated with the trans to gauche fatty chain change [23]. On the other hand, no change in the CH₂ scissoring band was observed, indicating no change in the packing structure of intercellular lipids [24]. Mitragotri et al. demonstrated that IL has a drug-dissolving effect, which could explain why 4MSK remained dissolved after water volatilization in this study [25]. Furthermore, SC fluidization is reversible and safe for the skin.

4.2. Transforming drugs into ILs

Firstly, we screened counter ions to convert 4MS to ILs, focusing on materials with basic functional groups, considering their interaction with the carboxyl groups of 4MS. At room temperature, 4MS combinations containing quaternary ammonium salts and some basic amino acids became liquid. The 4MS-Arg system was chosen for detailed physical property analysis from among the combinations in which 4MS became liquid. In this research, NMR,

IR, and DSC are used to characterize the physicochemical properties of ILs [7]. The results of ^{13}C -NMR and ^{15}N -HMBC spectra suggested that the carboxyl groups of 4MS dissociated to release H^+ . The chemical shifts of the first and third carbons of Arg, on the other hand, were shifted to higher fields, indicating that the carboxyl anion of Arg received proton (H^+) from 4MS. Furthermore, the chemical shift of Arg's -amino nitrogen in the IL was shifted to a lower magnetic field, indicating that Arg's NH_3^+ formed an ion pair with 4MS's carboxy anion. In summary, as shown in **Figure 6e**, it was fully confirmed that 4MS forms ion pairs with Arg. According to the results of solubility tests and NMR measurements of the system's supernatant with Arg excess, 4MS and Arg form a complex in aqueous solution at a molar ratio of 1:1. NEAT's ATR-IR results were completely consistent with NMR. It should be noted that the combination of Arg and 4MS resulted in an RT-IL. DSC measurements revealed that Arg-4MS is amorphous with a glass transition temperature, supporting the hypothesis that Arg-4MS evolved into ILs.

The lack of involvement of side chains in IL formation suggests that proton transfer is important in IL formation. It is generally believed that the “bulkiness” around the charged group and the difference in $\text{p}K_a$ are key to the ease of IL formation [25], and the structure of Arg and His and the balance of $\text{p}K_a$ may have contributed to the IL formation.

In addition, 4MS and Arg are used in industry to increase their water solubility in the form of potassium salts in the case of 4MS and hydrochloride salts in the case of arginine. Since the composition of the ions that form the skeleton is equivalent, it is important to check whether similar ILs are formed in aqueous solutions of 4MSK and ArgHCl. As a result, we confirmed the equivalence of the mixture of 4MSK and ArgHCl and Arg-4MS and found the same interaction in ArgHCl-4MSK as in Arg-4MS by using NMR. These findings suggest that this reaction is based on salt metathesis [26]. Furthermore, it should be noted that ArgHCl and 4MSK spontaneously form an IL of Arg-4MS even in an aqueous solution. In this study, ArgHCl-4MS was used for permeation experiments aiming at actual practical use. The flux, which represents the rate of transdermal penetration, was calculated and revealed that a simple mixture of 4MSK and ArgHCl increased the flux by 2.5 times when compared to a simple aqueous solution. The steady state flux generally reflects the partition coefficient of the drug to the SC and the subsequent diffusion coefficient in the SC [27]. The partition coefficients are determined by the molecule's hydrophobicity, while the diffusion coefficients

are determined by the molecule's size. It is assumed in this case that the macroscopic hydrophobicity increases with the formation of ILs. It's worth noting that the flux increased with Arg-4MS versus 4MSK, despite the apparent molecular weight increasing. ArgHCl-4MSK significantly accelerated skin penetration in human skin tests. In addition, the concentration in the SC increased due to IL formation even 4 hours after the concentration in the SC began to decrease, i.e., after T_{max} [10], suggesting that IL formation inhibits crystallization of 4MSK and efficiently forms a supersaturated state. Furthermore, it is well known that a compound's melting point and flux are inversely related [28-30], and the lower melting point due to IL formation may have contributed to the enhanced penetration.

Finally, we proposed “molecular modulation strategies” to be utilized for the effect enhancement of cosmetic drugs inspired by the potential of ILs. Molecular modulation strategies are approaches in which a complex (ILs) of cosmetic ingredients (parts) with an existing, non-new active changes physicochemical properties to produce a new effect, such as improved penetration (**Figure 8**). Our strategies for changing the ingredient properties without any chemical reaction demonstrated a significant improvement in skin permeation, which has great potential in cosmetic active drug delivery.

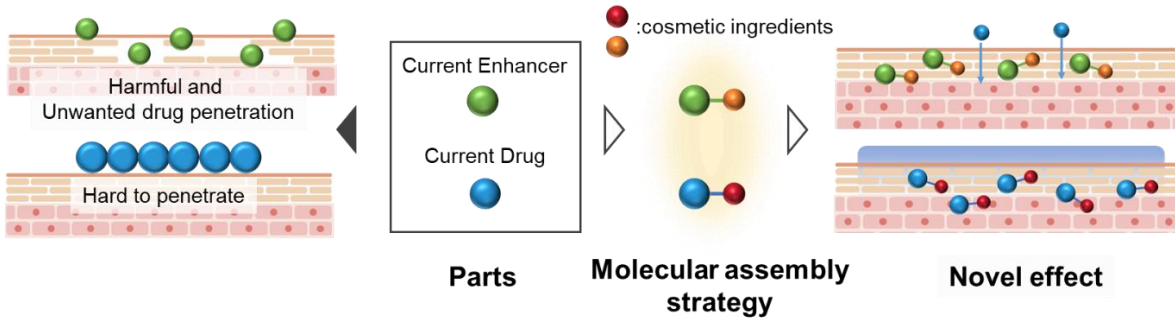


Figure 8 | Illustration of molecular modulation strategies.

Conventional enhancers cause toxicity or promote the penetration of dangerous compounds, and conventional drugs have too high melting points and are too hydrophilic to penetrate hydrophobic skin. These compounds are treated as parts and combined with other cosmetic ingredients to create skin penetration enhancers that are safe and effective, as well as having a lower melting point and higher hydrophobicity to increase penetration. By combining compounds, it is possible to make them behave as if they were new compounds.

5. Conclusion.

In this research, we have developed two novel ILs based on the molecular modulation strategies. For the first time, we developed the enhancer IL, AB/XY, and show the transdermal penetration enhancement of 4MSK. Furthermore, AB/XY may reduce AB toxicity. FT-IR is used to investigate the fundamental mechanism of significant penetration enhancement. We demonstrate the extraction and fluidization of SC lipid using AB/XY. Following that, we challenged ourselves to magically transform 4MS into IL, Arg-4MS. We show the overwhelming increment of 4MSK penetration by IL creation. Furthermore, Arg-4MS created IL by simply mixing 4MSK and ArgHCl. These technologies have the potential to go beyond cosmetics and help consumers stay healthy, beautiful, and age-free. As a non-invasive, safe, secure, and simple-to-use cosmetic procedure, such technology will improve the lives of consumer.

6. Acknowledgement

We would like to thank Mr. Norinobu Yoshikawa for helpful advice on FT-IR measurements. We are also grateful to Ms. Hiroko Manabe for helpful advice on quantitative analysis. Authors also sincerely thank Prof. Yasunari Iwao for fruitful discussion on the results.

7. Conflict of Interest Statement.

NONE.

8. References.

1. Stamford NPJ (2012) Stability, transdermal penetration, and cutaneous effects of ascorbic acid and its derivatives. *J Cosmet Dermatol* 11: 310–317.
2. Som I, Bhatia K, Yasir M (2012) Status of surfactants as penetration enhancers in transdermal drug delivery. *J Pharm Bioallied Sci* 4: 2–9.
3. Karande P et al (2005) Design principles of chemical penetration enhancers for transdermal drug delivery. *Proc Natl Acad Sci* 102(13): 4688-4693.
4. Ibsen KN, Tanner EEL, Mitragotri S (2019) Oral ionic liquid for the treatment of diet- induced obesity. *Proc Natl Acad Sci* 116(50): 25042-25047.

5. Banerjee A et al (2017) Transdermal Protein Delivery Using Choline and Geranate (CAGE) Deep Eutectic Solvent. *Adv Helthcare Mater* 6: 1601411.
6. Moshikur RM et al (2018) Characterization and cytotoxicity evaluation of biocompatible amino acid esters used to convert salicylic acid into ionic liquids. *Int J Pharm* 546: 31–38.
7. Wu X et al (2021) Ionic liquids as a useful tool for tailoring active pharmaceutical ingredients. *J Control Release* 338: 268–283.
8. Mitkare SS, Lakhane KG, Kokulwar PU (2013) Ionic liquids: Novel applications in drug delivery. *Res J Pharm Technol* 6: 1274–1278.
9. Abbott AP et al (2004) Deep Eutectic Solvents Formed between Choline Chloride and Carboxylic Acids : Versatile Alternatives to Ionic Liquids. *J Am Chem Soc* 9142–9147.
10. Sugibayashi K *Skin Permeation and Disposition of Therapeutic and Cosmeceutical Compounds*.
11. O'Brien J et al (2000) Investigation of the Alamar Blue (resazurin) fluorescent dye for the assessment of mammalian cell cytotoxicity. *Eur J Biochem* 267: 5421–5426.
12. Kligman AM, Christophers E (1963) Preparation of Isolated Sheets of Human Stratum Corneum *Arch Dermatol* 88: 702–705.
13. Clendennen SK, Boaz NW (Elsevier Inc., 2019). *Betaine Amphoteric Surfactants-Synthesis, Properties, and Applications. Biobased Surfactants: Synthesis, Properties, and Applications*.
14. Dai Y et al (2013) Natural deep eutectic solvents as new potential media for green technology. *Anal Chim Acta* 766: 61–68.
15. Wu W et al (2004) Desulfurization of flue gas: SO₂ absorption by an ionic liquid. *Angew Chemie Int Ed* 43: 2415–2417.
16. Kadhum WR et al (2017) A novel chemical enhancer approach for transdermal drug delivery with C17-monoglycerol ester liquid crystal-forming lipid. *J Oleo Sci* 66: 443–454.
17. Mulia K, Muhammad F, Krisanti E (2017) Extraction of vitexin from binahong (*Anredera cordifolia* (Ten.) Steenis) leaves using betaine - 1,4 butanediol natural deep eutectic solvent (NADES). *AIP Conf Proc* 1823: 020018.

18. Liu H et al (2004) Structural characterization and antimicrobial activity of chitosan/betaine derivative complex. *Carbohydr Polym* 55: 291–297.
19. McEwen AB et al (1999) Electrochemical Properties of Imidazolium Salt Electrolytes for Electrochemical Capacitor Applications. *J Electrochem Soc* 146: 1687–1695.
20. Moura Ramos JJ, Afonso CAM, Branco LC (2003) Glass transition relaxation and fragility in two room temperature ionic liquids. *J Therm Anal Calorim* 71: 659–666.
21. Effendy I, Maibach HI (1996) Detergent and skin irritation. *Clin Dermatol* 14: 15–21.
22. Qi QM, Mitragotri S (2019) Mechanistic study of transdermal delivery of macromolecules assisted by ionic liquids. *J Control Release* 311–312: 162–169.
23. Potts R, Guy RH (1991) Examination of the effect of ethanol on human stratum corneum in vivo using infrared spectroscopy. *J Control Release* 16: 299–304.
24. Goates CY, Knutson K (1994) Enhanced permeation of polar compounds through human epidermis. I. Permeability and membrane structural changes in the presence of short chain alcohols. *Biochim Biophys Acta* 1195: 169–179.
25. Stoimenovski J, Izgorodina EI, MacFarlane DR (2010) Ionicity and proton transfer in protic ionic liquids. *Phys Chem Chem Phys* 12: 10341–10347.
26. Balk A, Holzgrabe U, Meinel L (2015) Pro et contra' ionic liquid drugs - Challenges and opportunities for pharmaceutical translation. *Eur J Pharm Biopharm* 94: 291–304.
27. Kenji S et al (2004) Utility of a Three-Dimensional Cultured Human Skin Model as a Tool to Evaluate the Simultaneous Disposition and Metabolism of Ethyl Nicotinate in Skin. *Drug Metab Pharmacokinet* 19: 352–362.
28. Touitou E, Chow DD, Lawter JR (1994) Chiral β-blockers for transdermal delivery. *Int J Pharm* 104: 19–28.
29. Kasting GB et al (1987) Effect of lipid solubility and molecular size on percutaneous absorption The barrier function of the skin in relation to percutaneous absorption of drugs The effect of aging on percutaneous absorption in man A predictive algorithm for skin permeability. *Pharmacol Ski* 1: 138–153.